Thermal Conductivity Coefficients of Water and Heavy Water in the Liquid State up to 370 °C

B. Le Neindre,* P. Bury, R. Tufeu, and B. Vodar
Laboratoire des Interactions Moléculaires et des Hautes Pressions, C.N.R.S., 92190 Meudon-Bellevue, France

The thermal conductivity coefficients of water and heavy water of 99.75% isotopic purity were measured using a coaxial cylinder apparatus, covering room temperature to their critical temperatures, and pressures from 1 to 500 bar for water, and from 1 to 1000 bar for heavy water. Following the behavior of the thermal conductivity coefficient of water, which shows a maximum close to 135 °C, the thermal conductivity coefficient of heavy water exhibits a maximum near 95 °C and near saturation pressures. This maximum is displaced to higher temperatures when the pressure is increased. Under the same temperature and pressure conditions the thermal conductivity coefficient of heavy water was lower than for water. The pressure effect was similar for water and heavy water. In the temperature range of our experiments, isotherms of thermal conductivity coefficients were almost linear functions of density.

I. Introduction

Until recently, thermal conductivity coefficients of water and heavy water were measured and compared for limited temperature and pressure ranges.

The thermal conductivity coefficients of water in the liquid phase were determined at atmospheric or moderate pressure, by Challoner and Powell (*3*) up to 80 °C, Schmidt and Sellschopp (*10*), Vargaftik (*12, 15*), and Venart (*17*) up to 260 °C, Tarzimanov and Lozovoï (*11*) up to 154 °C and 1000 bar, Rastorguev (*9*) up to 180 °C and 2000 bar, and Minamiyama and Yata (*7*) in the same temperature and pressure ranges, and at higher pressure, by Bridgman (*1*) up to 12 000 kg/cm^2 and Lawson et al. (*5*) up to 8000 kg/cm^2.

The thermal conductivity coefficients of heavy water were carried out by Vargaftik et al. (*16*), near to the saturation curve. Ziebland and Burton, using a coaxial cylinder apparatus, studied temperatures ranging between 75 and 260 °C and pressures from 24 to 294 atm (*18*).

In this paper we report accurate measurements for the thermal conductivity coefficients of water and heavy water up to their critical temperatures.

II. Experimental Apparatus

(*1*) *Thermal Conductivity Cell.* As the critical pressure of water (221.2 bar) and heavy water (218.8 bar) are not too high, an external heating method was used. The high pressure vessel which maintained the cell at pressure was enclosed in a thermostat.

The cell of large size was tightened so that the water under investigation is confined in the vertical gap of the cell and is isolated from electrical wires. This ensures certain advantages: the initial purity of water is maintained, electrical measurements are not disturbed by physicochemical effects or conduction, the ionization is absent; consequently a good reproducibility of measurements is obtained.

A diagram of the cell is shown in Figure 1. The internal cylinder or emitter C_2 was 120 mm in length and 20 mm in diameter. The shape of the lower part was conical, with a 90° angle and 11 mm base. Five holes were drilled in the base, one along the axis contained the heating element and four others of different lengths, arranged symmetrically, used for thermocouples.

The external cylinder or receiver C_1 was 200 mm in length, 49 mm o.d. and 21 mm i.d. Surfaces of the gap were carefully polished. Five semicircular grooves, 2.5 mm wide and 2.5 mm deep, were bored in the circumference. At the ends of the grooves, holes were drilled obliquely to the external surface. They contained one thermocouple for temperature measurement and four thermocouples for temperature difference measurements. The distance between the thermocouple junction and the internal wall was 0.5 mm.

The internal cylinder C_2, soldered to a platinum–rhodium tube, was centered by means of the two cylinders G_1 and G_2. The centering of the lower part was achieved by four alumina pins A_1, machined at an angle of 90° and supported by a cone of the same angle on the centering piece G_2. A hole drilled in the upper part of the internal cylinder ensured that the center of the aluminum pin A_2 fitted into G_1. Platinum–iridium springs pushed on the centering pieces and prevented the displacement of the internal cylinder between the five alumina pins. Thermal insulation of the platinum–rhodium tube P was achieved by a sintered alumina cylinder A. The thickness of the liquid gap was 0.5 mm. The choice of this gap was a compromise between decreasing convection on one hand, and errors due to the wall wetness and accommodation on the other hand.

The 11.2 mm long heating element, set up in the internal cylinder, initiated the temperature difference between the cylinders. It was made of platinum–rhodium wire, 0.3 mm in diameter in the middle and 0.25 mm at each end to take into account end effects. Each length was calculated to dissipate the same energy per surface unit. These wires were helically wound around a 4 mm o.d. aluminum tube, with a groove having a 0.6 mm pitch, imbedded in alumina cement. Four gold wires soldered at the resistor terminals were used to measure the power supplied to the internal cylinder. A dc generator provided a well-stabilized current to the resistor.

The temperature difference between the two cylinders was measured by eight thermocouples in series, placed suitably along the wall to minimize the inhomogeneities of temperature.

A thermocouple set up in the external cylinder gave the temperature of the experiment and an ice bath provided the zero temperature reference. All thermocouples were in platinum/platinum 10% rhodium and were isolated by alumina tubes. Electromotive forces at the thermocouple terminals and power at the resistor terminals were measured by a Leeds and Northrup potentiometer.

(*2*) *High Pressure Apparatus.* This study was performed under pressure in order to take into account the increase of the saturation pressure with the temperature, but also to study the pressure effects on the thermal conductivity. The high pressure vessel containing the cell was heated by a thermostatic bath (Figure 2). Due to the great modifications of the experimental conditions there was a thermal expansion of the fluid filling the cell. A bellows, set up in the upper part of the high pressure vessel and maintained at room temperature, was used to compensate the volume variations and to balance the pressure between the sample and the compressing fluid. Gaseous nitrogen was the fluid compressor.

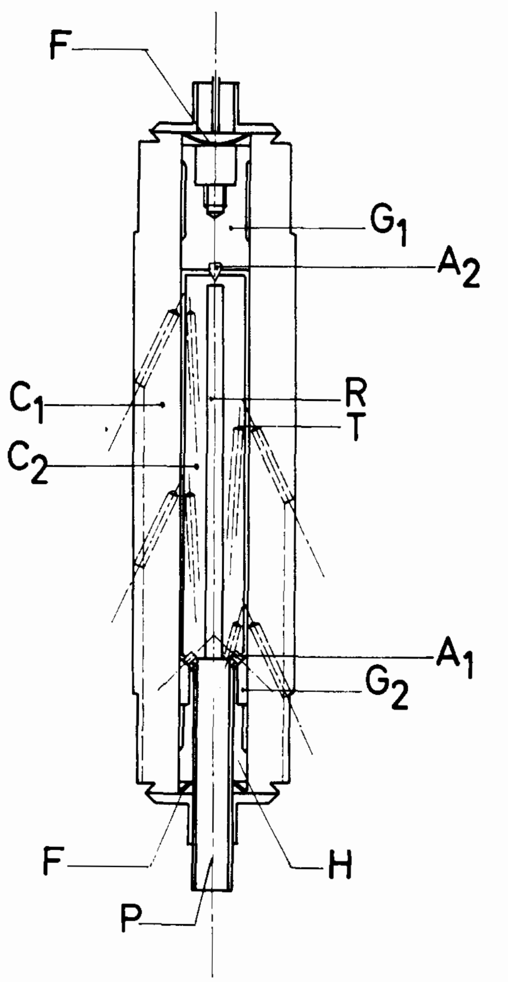

Figure 1. Thermal conductivity cell: C_1, external cylinder; C_2, internal cylinder; G_1 and G_2, centering cylinders; A, alumina pins; R, resistor; F, spring; P, platinum–rhodium tube; H, isolating piece in alumina.

The lower element 3 was also kept at room temperature. It was composed of a high pressure head in which eight holes were drilled for conical feedthroughs isolated by 0.2–0.3 mm thick conical Teflon sleeves. Four of these feedthroughs were soldered to thermocouples, the others were soldered to wires used for voltage and current measurements. The elements 1, 2, and 3, were made of Valimphy steel of tensile strength 65 kg/mm^2. Tubings and connections were made of Imphy 1691 of tensile strength 85 kg/mm^2 and the remaining elements of NCT 10 steel having a tensile strength of 65 kg/mm^2. All these steels were provided by Imphy Co. All seals were of the insupported area type.

(3) Thermostat. The double-walled thermostat using a circulation of organic liquid under a pressure of 6 bar was used up to 370 °C. The thermofluid was preheated before being forced into the thermostat by a centrifugal pump. The preheating was performed by six resistors isolated from the metallic container by magnesa. Two resistors were connected to a temperature controller, three others were controlled by hand and worked at full power (4 kW). The power emitted by the sixth was adjusted between 0 and 1 kW by means of an autotransformer.

The temperature-sensitive element was a 27.6 Ω at 22 °C resistance thermometer, set up in the wall of the high pressure apparatus. A thyratron temperature controller controlled the temperature.

Good conditions of stability and homogeneity of temperature were reached easily. Temperature fluctuations of the cell were less than 0.01 °C throughout the temperature range.

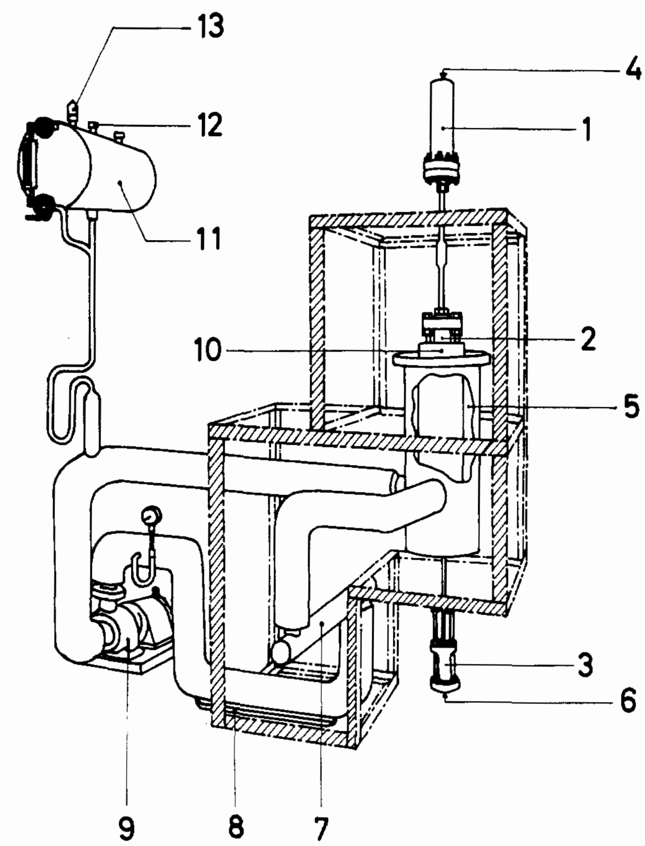

Figure 2. Thermostat and high pressure apparatus: (1–3) high pressure apparatus, (4) compressor gas input, (5) thermostat, (6) electrical feedthroughs, (7) electrical heater, (8) by-pass, (9) pump, (10) high pressure vessel, (11) expansion vessel, (12) compressing gas input, (13) relieve valve.

III. Experimental Methods

The thermal conductivity coefficient was deduced from measurements of heat Q transmitted radially across the fluid layer, the temperature difference ΔT between the two cylinders, and the thickness of the fluid layer, by the relation:

$$\lambda = K\frac{Q}{\Delta T} \quad (1)$$

(1) Measurement of the Geometrical Constant. According to the formal equations which govern the electric field and the thermal field, the cell is analogous to a capacitor. The calibration of the cell has been previously described (*13*). It is performed prior to the soldering of the end pieces. The cell is placed vertically, and the capacitances of both internal cylinder and platinum–rhodium tube were measured. Then, these elements were removed and the capacitance of a metallic tube, set up in the same position as the platinum–rhodium tube, was determined. The capacitance of the cell was deduced from these two measurements. Capacitances were measured at a frequency of 500 kHz in a capacitance bridge by comparison to a standard capacitance. A correction was made to take into account the dielectric constant of the alumina pins. The effective capacitance in air after correction was 133.1 ± 0.3 pF at 20 °C.

The geometrical constant was calculated by

$$K = \frac{\epsilon_0\epsilon_r}{C} = \frac{8.8541735 \times 1.00057}{133.1} = 0.066563 \quad (2)$$

The variation of the geometrical constant with temperature was taken into account by the relation:

$$K_t = \frac{K}{1 + k(T - 20)} \quad (3)$$

(2) Corrections. The heat emitted in the internal cylinder was transmitted to the external cylinder by conduction but also radiation through the fluid and by conduction through isolating pins, thermocouples, and wires used in the measurement of the power.

(a) Correction for the "Parallel" Heat Transfer. This correction takes into account the heat transfer by the isolating pins and wires used in power measurements, and one part of the heat transmitted by radiation. Previously some authors determined the parallel heat transfer by differential measurement under vacuum conditions, but we found experimentally that the thermal contact resistance between silver and aluminum was a function of the thermal conductivity of the studied fluid (*13*). Then we calibrated the cell with a gas of known thermal conductivity. Helium was chosen because of its high thermal conductivity. The calibration was made at a pressure of 100 bar to avoid corrections due to the accommodation effect. The experimental data were compared to those of Johannin et al. (*4*). The parallel heat transfer was found to be nearly constant and equal to 0.015 W $m^{-1}\,{}^{\circ}C^{-1}$.

(b) Heat Transfer by Radiation. We studied the influence of the wall emissivity on the conductive heat transfer. The experiment was performed at room temperature. A black silver sulfide layer was deposited on the wall. We observed slightly lower values of the thermal conductivity (1%), which seemed to be due to a perturbation of the temperature difference of isolating layers of silver sulfide.

For a fluid completely transparent to thermal radiations, a good approximation of the heat transfer by radiation is:

$$Q_r = \alpha\sigma S 4 T^3 \Delta T \qquad (4)$$

The silver cylinders were perfectly polished, their emissivity was small and Q_r (calculated by eq 4) is negligible by comparison with the heat transfer by conduction in the temperature range of our experiment. Moreover, Q_r as defined was taken into account in the parallel heat transfer correction. Although the heat transfer by radiation could be higher in a fluid exhibiting specific absorption than in a transparent fluid (as pointed out by Poltz (*8*)), the correction accounting for this absorption is small for water at room temperature (*8*) and we assumed it negligible up to the critical temperature.

(c) Correction for the Convection Heat Transfer. The generalization of heat transfer measurements between coaxial cylinders shows that the convection regime is related to the Rayleigh number:

$$R = G_r P_r = \frac{g\beta\rho^2 C_p d^3 \Delta T}{\eta\lambda} \qquad (5)$$

In the critical region, due to the increasing of β and C_p, the Rayleigh number increases rapidly.

At temperatures higher than 300 °C where the Rayleigh number is not negligible, the convection heat transfer is calculated by the following equation:

$$Q_{cv} = R\frac{\lambda\Delta T}{720} 2\pi r \qquad (6)$$

Such calculations give only a rough estimate of the convection. In fact we did not precisely know the variation of most of the quantities in eq 5. Corrections were always less than 1.8%, the most important being found for heavy water at 350 °C and 202.6 bar. Let us remark that for $R = 1000$ which was considered as a criterium for the beginning of convection, formula 6 shows that 0.6% of the heat was transferred by convection.

(d) Corrections for Thermocouple Positions. Temperatures and temperature differences were measured at the silver wall and not in the fluid, thus it was necessary to take into account the temperature gradient in the cell wall. This correction is given by:

$$\lambda_{corr} = \lambda_{measd}\left(1 + \frac{D}{\lambda_s d}\lambda_{measd}\right) \qquad (7)$$

An analogous study between potential fields and temperature fields shows that isotherms are distorted in the vicinity of the

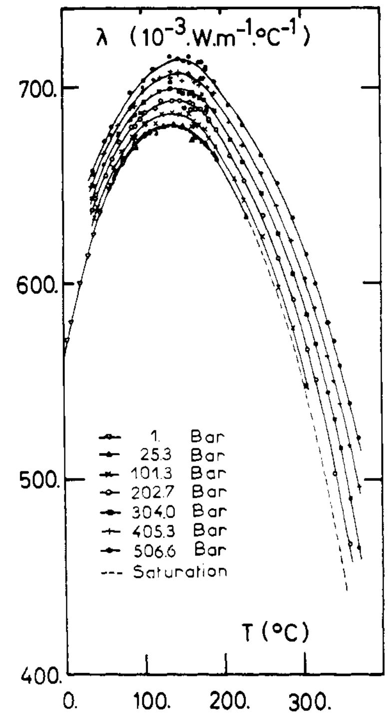

Figure 3. Thermal conductivity coefficients of water.

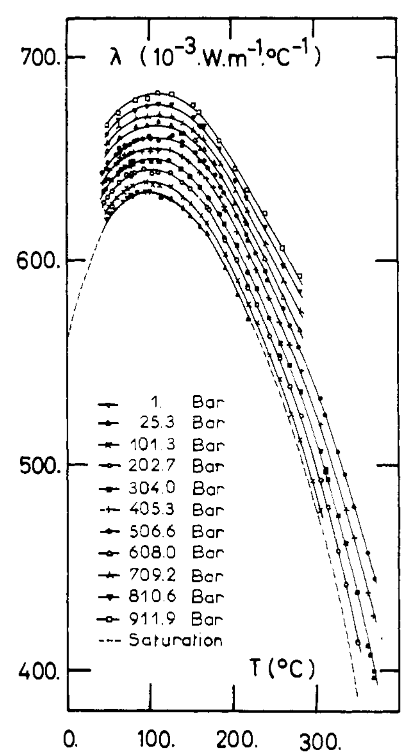

Figure 4. Thermal conductivity coefficients of heavy water.

Table I. Thermal Conductivity Coefficients of Water

10^{-5} *P*, N m^{-2}	*ρ*, kg/m^3	*T*, °C	λ, W m^{-1} °C^{-1}	10^{-5} *P*, N m^{-2}	*ρ*, kg/m^3	*T*, °C	λ, W m^{-1} °C^{-1}
202.7	1001.7	37.5	0.6376	405.3	960.2	122.7	0.7046
304.0	1006.1	37.2	0.6432	101.3	943.8	124.9	0.6864
304.0	1006.1	37.5	0.6437	101.3	943.8	125.0	0.6859
405.3	1010.4	37.3	0.6500	25.3	938.3	126.0	0.6805
506.6	1014.4	37.2	0.6550	25.3	927.6	139.7	0.6817
506.6	1014.6	36.8	0.6530	101.3	931.9	139.0	0.6876
506.6	1014.3	37.5	0.6575	202.7	938.0	138.1	0.6932
405.3	1009.9	38.7	0.6537	304.0	943.8	137.4	0.6994
405.3	1009.4	39.6	0.6544	405.3	949.2	136.6	0.7045
304.0	1004.8	40.9	0.6509	506.6	954.2	136.2	0.7106
202.7	1001.1	42.2	0.6455	506.6	954.4	136.0	0.7151
202.7	1000.0	42.3	0.6434	405.3	949.1	136.7	0.7078
101.3	994.7	44.5	0.6387	304.0	944.0	137.1	0.7024
25.3	990.5	46.8	0.6360	202.7	938.3	137.7	0.6932
25.3	984.0	60.5	0.6501	101.3	932.2	138.6	0.6861
25.3	982.3	63.6	0.6541	25.3	927.7	139.4	0.6817
101.3	985.2	64.2	0.6587	405.3	940.6	147.1	0.7076
202.7	994.4	54.7	0.6550	405.3	940.6	147.1	0.7068
304.0	1000.0	51.8	0.6612	506.6	945.7	146.7	0.7139
405.3	1003.4	53.4	0.6666	304.0	935.1	147.6	0.6976
506.6	1008.0	52.4	0.6723	202.7	929.3	148.2	0.6924
506.6	1003.6	61.0	0.6796	101.3	922.8	149.0	0.6859
405.3	999.4	61.5	0.6751	25.3	918.4	149.7	0.6783
304.0	995.0	62.1	0.6685	506.6	941.4	151.8	0.7131
202.7	990.2	63.0	0.6631	405.3	936.2	152.2	0.7031
101.3	984.8	65.0	0.6593	304.0	930.6	152.7	0.6970
25.3	980.8	66.5	0.6556	202.7	924.6	153.2	0.6891
5.1	979.7	66.8	0.6571	304.0	923.9	160.2	0.6975
202.7	985.5	71.6	0.6713	202.7	917.6	160.8	0.6920
304.0	990.4	70.7	0.6756	202.7	918.1	160.3	0.6923
304.0	990.4	70.7	0.6767	101.3	911.7	161.0	0.6864
405.3	994.8	70.0	0.6807	25.3	906.7	161.7	0.6794
2.0	974.8	75.3	0.6629	405.3	911.5	161.2	0.7028
101.3	980.0	73.6	0.6674	405.3	929.8	159.4	0.7077
25.3	976.0	74.9	0.6632	405.3	925.4	164.3	0.7048
202.7	976.3	87.1	0.6793	304.0	919.7	164.6	0.6974
101.3	971.0	88.4	0.6751	202.7	913.4	165.2	0.6912
25.3	966.7	89.6	0.6710	101.3	906.8	166.0	0.6825
304.0	981.2	86.3	0.6832	25.3	902.0	166.5	0.6769
405.3	985.6	85.7	0.6895	506.6	934.1	160.3	0.7118
506.6	990.4	84.7	0.6972	506.6	934.3	160.1	0.7153
5.1	965.6	89.9	0.6721	405.3	928.8	160.6	0.7066
405.3	982.7	90.5	0.6906	304.0	923.0	161.1	0.6967
405.3	982.6	90.6	0.6920	202.7	916.7	161.8	0.6878
304.0	978.2	91.0	0.6856	101.3	910.1	162.6	0.6797
202.7	973.3	91.7	0.6796	25.3	905.3	163.1	0.6733
101.3	968.0	92.9	0.6743	101.3	904.7	168.1	0.6806
25.3	963.8	93.9	0.6691	25.3	899.8	168.7	0.6743
5.1	955.4	104.3	0.6758	405.3	923.6	166.2	0.7022
25.3	956.4	104.2	0.6757	304.0	917.6	166.8	0.6956
101.3	960.2	103.9	0.6810	202.7	911.3	167.4	0.6883
202.7	968.8	98.3	0.6834	25.3	893.4	174.8	0.6723
304.0	973.6	98.0	0.6868	25.3	892.9	175.2	0.6724
405.3	975.0	102.3	0.6935	101.3	898.1	174.6	0.6804
506.6	979.5	101.8	0.7003	202.6	905.1	173.9	0.6885
304.0	969.6	103.8	0.6921	304.0	911.5	173.3	0.6943
405.3	974.5	103.1	0.6983	405.3	917.3	173.1	0.7011
506.6	979.0	102.5	0.7032	506.6	923.4	172.5	0.7111
202.7	964.4	104.6	0.6866	506.6	923.4	172.4	0.7121
101.3	958.8	105.8	0.6814	405.3	917.6	172.9	0.7030
25.3	954.4	106.8	0.6767	506.6	921.0	175.1	0.7120
15.2	954.0	106.8	0.6769	405.3	915.3	175.4	0.7044
5.1	953.6	106.8	0.6756	304.0	909.2	175.7	0.6937
25.3	945.8	118.1	0.6767	304.0	908.2	176.7	0.6931
25.3	945.5	118.5	0.6780	304.0	907.4	177.6	0.6940
101.3	949.8	117.6	0.6816	304.0	906.2	178.7	0.6936
202.7	955.4	116.7	0.6890	304.0	905.1	180.0	0.6938
506.6	970.3	115.0	0.7091	25.3	886.8	181.0	0.6713
405.3	965.7	115.4	0.7038	101.3	892.1	180.6	0.6784
202.7	949.6	124.1	0.6928	202.6	899.2	179.9	0.6863
304.0	955.8	123.2	0.6983	304.0	907.4	177.6	0.6967

Table I. Continued

10^{-5} P, N m^{-2}	ρ, kg/m^3	T, °C	λ, W m^{-1} °C^{-1}	10^{-5} P, N m^{-2}	ρ, kg/m^3	T, °C	λ, W m^{-1} °C^{-1}
405.3	913.7	177.0	0.7045	202.6	786.9	270.3	0.6127
25.3	888.7	179.3	0.6724	101.3	772.8	270.8	0.5976
506.6	916.2	180.5	0.7081	101.3	739.6	288.8	0.5769
506.6	916.3	180.3	0.7093	202.6	756.8	288.5	0.5913
405.3	909.5	181.5	0.7001	101.3	739.6	288.8	0.5767
304.0	902.8	182.3	0.6904	304.0	771.4	288.2	0.6049
304.0	902.8	182.3	0.6881	405.3	784.4	288.1	0.6218
202.6	895.7	183.2	0.6830	506.6	795.1	287.9	0.6331
202.6	895.8	183.1	0.6835	506.6	771.0	304.6	0.6146
101.3	888.4	184.0	0.6742	405.3	758.2	304.9	0.6024
101.3	877.7	193.9	0.6698	304.0	742.9	305.1	0.5844
405.3	899.0	192.2	0.6972	206.6	724.6	305.5	0.5660
25.3	871.6	194.5	0.6638	101.3	701.8	305.7	0.5474
304.0	892.5	192.6	0.6882	202.6	662.2	331.8	0.5180
202.6	885.2	193.3	0.6783	304.0	690.6	331.5	0.5421
506.6	905.2	191.9	0.7022	405.3	711.7	331.3	0.5612
405.3	880.5	210.2	0.6817	506.6	727.8	331.2	0.5792
202.6	865.7	211.1	0.6650	506.6	713.7	339.0	0.5695
304.0	873.3	210.6	0.6731	505.6	713.7	339.0	0.5699
505.6	888.0	209.8	0.6906	405.3	697.8	339.2	0.5481
405.3	862.7	226.4	0.6703	304.0	672.5	339.4	0.5290
506.6	870.2	226.0	0.6802	202.6	639.0	339.6	0.4985
304.0	854.6	226.8	0.6622	506.6	699.8	346.7	0.5575
202.6	846.2	227.2	0.6521	405.3	683.1	346.8	0.5363
101.3	837.3	227.6	0.6422	304.0	652.7	347.0	0.5133
27.6	830.1	228.0	0.6350	202.6	611.6	347.3	0.4818
101.3	804.2	251.3	0.6235	506.6	653.6	369.5	0.5204
101.3	804.4	251.2	0.6238	405.3	624.2	369.7	0.4955
202.6	815.4	250.8	0.6345	304.0	580.3	369.9	0.4631
304.0	825.7	250.3	0.6459	202.6	699.7	317.2	0.5486
405.3	834.9	250.0	0.6565	304.0	720.5	317.0	0.5675
506.6	843.2	249.7	0.6651	405.3	738.0	316.9	0.5840
506.6	818.3	269.3	0.6513	506.6	752.4	316.7	0.5995
506.6	818.3	269.3	0.6510	506.6	676.6	358.5	0.5380
405.3	809.7	269.6	0.6396	405.3	653.2	358.6	0.5153
304.0	799.2	270.0	0.6256	304.0	619.2	358.8	0.4862
304.0	799.2	270.0	0.6250				

thermocouple holes, but that there is an identity between measured temperature and axial temperature in the holes. (In our case $D = 4.0$ mm; $d = 0.5$ mm, $\lambda_s = 420$ W m^{-1} °C^{-1}, giving $D/\lambda_s d = 0.019$.)

(e) Precision Estimates of Measurements. Water and heavy water were degassed under vacuum. Heavy water had an isotopic purity of 99.75%. Errors due to impurities were therefore negligible. The precision of the pressure measurement was ±0.7 bar. The calibration of thermocouples with a standard platinum resistor gave an error of ±0.2 °C by comparison with the international scale. We consider that the error in temperature was less than ±0.3 °C. The correction due to the compressibility of silver was negligible since the entire cell was under pressure.

The accuracy of the potentiometer was better than the other sources of errors. The error in the temperature difference was less than 0.4%.

The error in the conversion of voltage to temperature was less than 0.2%.

The error on the power measurement was less than 0.01%. The error on the geometrical constant determined from electrical capacitance measurements leads to an uncertainty of 0.22% in the thermal conductivity.

The error on the parallel heat transfer depends upon the precision of the measurements of the thermal conductivity of helium. We assumed the thermal conductivity of helium to be known within an error of 1.5%, so that the error of the thermal conductivity was less than 0.3%. The error in the Rayleigh number was estimated at 10%, leading to an error of 12% in the convective heat transfer and 0.2% in the thermal conductivity.

All of the other errors were assumed negligible. The total error was less than 1.50%.

IV. Results

Measurements were made at fixed temperatures, between room and the critical temperatures and at various pressures up to 500 bar. For heavy water another set of data was obtained between room temperature and 180 °C and up to 1000 bar (Tables I–IV and Figures 3 and 4).

(1) Comparison between the Thermal Conductivity of Water and Heavy Water. The thermal conductivity of water plotted as a function of temperature increases to a maximum at 135 °C for the saturation pressure. The thermal conductivity of heavy water also increases with temperature, but the maximum is at a lower temperature (95 °C). The dispersion of our data is small and it is possible to detect a displacement of the maximum to higher temperatures when the pressure increases.

A comparison, between thermal conductivity coefficients of water and heavy water up to 500 bar, shows the following: (a) The ratio D_2O/H_2O seems to be independent of pressure in the range of this study. (b) The thermal conductivity coefficient of water is always less than the thermal conductivity coefficient of heavy water.

By analogy to the kinematic viscosity, η, we define a volumic conductivity λ/ρ. Variations of the volumic conductivity in terms

Table II. Thermal Conductivity Coefficients of Heavy Water

10^{-5} *P*, N m^{-2}	*ρ*, kg/m^3	*T*, °C	λ, W m^{-1} °C^{-1}	10^{-5} *P*, N m^{-2}	*ρ*, kg/m^3	*T*, °C	λ, W m^{-1} °C^{-1}
1.0	1096.3	48.3	0.6207	506.6	1102.3	81.1	0.6581
101.3	1101.8	46.6	0.6243	405.3	1096.9	81.4	0.6534
202.7	1107.2	45.1	0.6295	202.7	1086.1	83.0	0.6416
304.0	1112.1	44.3	0.6343	202.7	1086.1	83.0	0.6424
506.6	1122.2	42.6	0.6417	506.6	1095.4	91.5	0.6595
506.6	1122.2	42.6	0.6406	506.6	1095.4	91.5	0.6592
506.6	1122.2	42.6	0.6431	405.3	1090.2	91.8	0.6531
405.3	1117.1	43.6	0.6379	403.3	1090.0	91.9	0.6536
506.6	1120.3	47.3	0.6448	304.0	1084.5	92.4	0.6484
405.3	1115.1	48.3	0.6400	304.0	1084.5	92.4	0.6481
405.3	1115.1	48.3	0.6393	202.7	1079.0	93.1	0.6445
304.0	1110.1	48.9	0.6356	202.7	1079.0	93.1	0.6445
304.0	1110.1	48.9	0.6349	101.3	1073.3	93.9	0.6382
202.7	1105.2	49.8	0.6315	1.0	1067.3	95.0	0.6337
202.7	1105.2	49.8	0.6298	101.3	1065.6	103.9	0.6368
202.7	1105.2	49.8	0.6312	202.7	1071.4	103.0	0.6422
101.3	1099.9	51.0	0.6267	304.0	1077.2	102.3	0.6490
101.3	1099.9	51.0	0.6261	506.6	1088.4	101.4	0.6588
25.3	1095.7	52.1	0.6211	405.3	1083.1	101.6	0.6541
1.0	1094.3	52.6	0.6227	405.3	1083.1	101.6	0.6549
1.0	1092.6	56.2	0.6258	405.3	1083.1	101.6	0.6535
1.0	1092.6	56.2	0.6255	506.6	1081.3	111.1	0.6585
101.3	1097.9	54.8	0.6281	506.6	1081.3	111.1	0.6592
202.7	1103.3	53.5	0.6337	506.6	1081.3	111.0	0.6585
304.0	1108.1	52.7	0.6398	405.3	1075.6	111.4	0.6542
405.3	1113.3	52.0	0.6448	304.0	1069.6	111.9	0.6486
506.6	1118.6	51.3	0.6478	202.7	1063.6	112.6	0.6431
506.6	1118.6	51.3	0.6482	101.3	1057.8	113.1	0.6372
506.6	1113.6	61.1	0.6521	25.3	1053.3	113.6	0.6320
405.3	1108.7	61.1	0.6467	25.3	1053.3	113.6	0.6314
405.3	1108.7	61.1	0.6480	25.3	1041.2	126.9	0.6301
405.3	1108.7	61.1	0.6477	25.3	1041.2	126.9	0.6304
304.0	1103.7	61.7	0.6429	101.3	1045.7	126.7	0.6364
304.0	1103.7	61.7	0.6419	202.7	1051.9	126.0	0.6430
202.7	1098.6	62.6	0.6384	304.0	1058.2	125.4	0.6491
506.6	1112.1	64.2	0.6536	405.3	1064.3	124.9	0.6540
506.6	1112.1	64.2	0.6534	506.6	1070.3	124.5	0.6598
506.6	1112.1	64.2	0.6534	506.6	1058.0	138.5	0.6561
405.3	1106.8	64.7	0.6498	405.3	1052.1	138.7	0.6507
405.3	1106.8	64.7	0.6503	304.0	1045.7	139.2	0.6447
405.3	1106.8	64.7	0.6509	304.0	1045.7	139.2	0.6442
304.0	1101.8	65.2	0.6447	304.0	1045.7	139.2	0.6438
506.6	1108.9	70.0	0.6555	304.0	1045.7	139.2	0.6448
506.6	1108.9	70.0	0.6562	202.7	1039.2	139.6	0.6379
405.3	1103.8	70.3	0.6505	101.3	1032.7	140.2	0.6313
405.3	1103.8	70.3	0.6519	25.3	1027.9	140.5	0.6262
304.0	1092.4	71.1	0.6460	25.3	1027.9	140.5	0.6256
202.7	1093.2	71.7	0.6410	25.3	1017.7	150.3	0.6226
101.3	1087.5	73.2	0.6354	101.3	1022.9	149.8	0.6278
25.3	1083.2	74.1	0.6307	202.7	1029.4	149.5	0.6351
1.0	1082.0	74.2	0.6303	304.0	1036.0	149.0	0.6414
1.0	1085.0	68.6	0.6285	405.3	1042.6	148.7	0.6479
101.3	1094.9	60.5	0.6307	506.6	1049.4	148.2	0.6542
506.6	1105.4	75.9	0.6562	506.6	1037.5	160.6	0.6489
506.6	1105.4	75.9	0.6565	405.3	1030.6	160.9	0.6422
405.3	1100.0	76.5	0.6527	405.3	1030.6	160.9	0.6429
304.0	1094.7	77.2	0.6466	304.0	1023.7	161.2	0.6358
304.0	1094.7	77.2	0.6487	101.3	1009.3	162.1	0.6220
202.7	1089.3	78.1	0.6414	25.3	1004.1	162.6	0.6170
202.7	1089.3	78.1	0.6413	25.3	995.7	170.0	0.6133
202.7	1089.3	78.1	0.6428	101.3	1001.0	169.8	0.6188
202.7	1089.3	78.2	0.6432	202.7	1007.8	169.9	0.6256
202.7	1089.3	78.3	0.6419	202.7	1005.8	171.8	0.6250
101.3	1083.6	79.4	0.6373	304.0	1012.8	171.5	0.6323
25.3	1079.3	80.2	0.6321	304.0	1012.8	171.5	0.6331
1.0	1077.7	80.8	0.6317	506.6	1027.3	171.0	0.6460
1.0	1074.9	84.7	0.6326	506.6	1027.3	171.0	0.6448
1.0	1074.9	84.7	0.6330	506.6	1007.6	190.1	0.6329
101.3	1080.5	83.9	0.6386	405.3	999.7	190.3	0.6243
202.7	1086.2	82.8	0.6428	405.3	999.7	190.3	0.6263
304.0	1091.6	82.1	0.6476	405.3	999.7	190.3	0.6237
304.0	1091.6	82.1	0.6490	304.0	992.1	190.3	0.6182

Table II. Continued

10^{-5} P, N m^{-2}	ρ, kg/m^3	T, °C	λ, W m^{-1} °C^{-1}	10^{-5} P, N m^{-2}	ρ, kg/m^3	T, °C	λ, W m^{-1} °C^{-1}
202.7	984.2	190.7	0.6106	506.6	843.2	312.0	0.5235
202.7	984.2	190.7	0.6092	304.0	771.6	327.6	0.4732
101.3	976.1	191.0	0.6027	304.0	771.6	327.6	0.4736
101.3	976.1	191.0	0.6034	202.7	743.4	327.6	0.4550
25.3	970.0	191.2	0.5966	506.6	816.3	326.8	0.5059
25.3	951.1	205.8	0.5829	202.7	743.4	327.6	0.4544
25.3	951.1	205.8	0.5843	506.6	775.2	346.7	0.4787
101.3	957.5	205.9	0.5907	405.3	750.2	346.7	0.4618
202.7	965.8	205.8	0.5998	304.0	709.2	349.9	0.4351
304.0	974.3	205.7	0.6074	304.0	709.2	349.9	0.4359
405.3	982.5	205.7	0.6141	202.7	655.3	350.2	0.4056
506.6	991.3	205.4	0.6222	506.6	775.2	346.7	0.4793
506.6	991.3	205.4	0.6210	405.3	750.2	346.7	0.4622
506.6	977.5	218.2	0.6100	202.7	655.3	350.2	0.4063
506.6	977.5	218.2	0.6093	202.7	714.3	336.0	0.4372
405.3	968.2	218.3	0.6017	202.7	714.3	336.0	0.4378
304.0	959.3	218.4	0.5944	304.0	750.2	335.9	0.4598
304.0	959.3	218.4	0.5937	405.3	776.2	335.7	0.4767
202.7	950.2	218.5	0.5868	506.6	798.0	335.7	0.4945
202.7	950.2	218.5	0.5861	506.6	738.0	362.8	0.4561
101.3	940.6	218.8	0.5784	405.3	706.7	362.8	0.4337
25.3	933.0	219.0	0.5717	304.0	664.0	362.7	0.4093
101.3	925.6	229.6	0.5689	304.0	659.6	363.8	0.4097
101.3	925.6	229.6	0.5683	405.3	704.1	363.6	0.4351
202.7	935.8	229.5	0.5777	506.6	735.3	363.6	0.4570
304.0	945.9	229.1	0.5867	506.6	720.9	369.2	0.4441
405.3	955.7	228.9	0.5952	405.3	687.8	369.5	0.4232
506.6	967.5	228.7	0.6035	304.0	636.5	369.9	0.3938
506.6	947.1	243.8	0.5902	202.7	774.5	316.7	0.4766
405.3	938.2	244.0	0.5815	304.0	801.9	314.3	0.4916
304.0	925.3	244.1	0.5719	202.7	895.1	256.4	0.5531
202.7	914.4	244.2	0.5626	103.3	881.0	256.7	0.5418
101.3	902.5	244.5	0.5534	101.3	881.0	256.6	0.5415
101.3	880.3	257.1	0.5405	506.6	1112.5	63.5	0.6552
202.7	893.7	257.1	0.5506	608.0	1117.7	63.1	0.6601
304.0	905.7	257.1	0.5604	709.2	1122.8	62.8	0.6665
405.3	917.4	256.8	0.5699	951.5	1134.0	62.1	0.6738
405.3	917.4	256.8	0.5693	911.9	1132.4	62.2	0.6726
506.6	929.4	256.6	0.5811	810.6	1127.6	62.6	0.6693
506.6	911.6	268.8	0.5676	506.6	1195.7	49.2	0.6477
506.6	911.6	268.8	0.5682	911.9	1138.9	49.0	0.6665
405.3	899.2	269.0	0.5584	810.6	1133.3	49.3	0.6617
304.0	885.7	269.1	0.5481	709.2	1129.3	49.6	0.6579
304.0	885.7	269.1	0.5487	608.0	1124.1	50.0	0.6538
202.7	871.8	269.4	0.5377	810.6	1115.8	82.9	0.6740
101.3	855.4	269.7	0.5246	810.6	1115.8	82.9	0.6738
101.3	772.8	306.4	0.4772	709.2	1111.1	83.0	0.6705
202.7	800.0	306.4	0.4916	608.0	1106.1	83.4	0.6658
304.0	817.7	306.4	0.5070	1001.0	1123.2	82.2	0.6829
405.3	835.4	306.3	0.5198	1001.0	1123.3	82.2	0.6822
405.3	835.4	306.3	0.5193	911.9	1120.4	82.4	0.6784
506.6	853.2	306.1	0.5321	810.6	1116.1	82.6	0.6745
202.7	800.0	306.4	0.4948	506.6	1100.7	83.7	0.6587
202.7	800.0	306.4	0.4945	506.6	1089.4	98.9	0.6612
506.6	871.1	295.2	0.5426	968.0	1112.6	97.1	0.6822
405.3	854.7	295.5	0.5321	968.0	1112.6	97.1	0.6811
304.0	838.2	295.6	0.5198	911.9	1110.2	97.4	0.6798
202.7	821.7	295.6	0.5066	810.6	1105.6	97.8	0.6756
202.7	821.7	295.6	0.5056	709.2	1100.9	98.0	0.6709
101.3	800.0	295.8	0.4911	608.0	1096.0	98.4	0.6663
101.3	800.0	295.8	0.4917	810.6	1096.1	110.9	0.6768
101.3	800.0	295.8	0.4924	998.4	1104.2	110.3	0.6853
101.3	826.4	282.8	0.5111	998.4	1104.2	110.3	0.6846
202.7	846.7	282.9	0.5238	911.9	1100.7	110.6	0.6822
304.0	862.0	282.8	0.5358	709.2	1091.6	111.1	0.6722
405.3	876.4	282.8	0.5462	608.0	1086.4	111.5	0.6678
506.6	891.2	282.5	0.5554	979.0	1090.9	126.3	0.6848
506.6	843.2	312.0	0.5242	911.9	1087.9	126.5	0.6818
405.3	825.1	312.3	0.5120	810.6	1083.4	126.7	0.6762
304.0	805.8	312.4	0.4981	709.2	1078.5	127.0	0.6714
304.0	803.2	313.7	0.4959	608.0	1073.8	127.4	0.6667
202.7	781.9	313.8	0.4780	506.6	1067.3	127.8	0.6611

Table II. Continued

10^{-5} P, N m^{-2}	ρ, kg/m^3	T, °C	λ, W m^{-1} °C^{-1}	10^{-5} P, N m^{-2}	ρ, kg/m^3	T, °C	λ, W m^{-1} °C^{-1}
779.1	1070.3	139.8	0.6723	608.0	1062.1	140.2	0.6627
785.9	1071.1	139.7	0.6718	506.6	1056.3	140.6	0.6561
304.0	996.3	186.5	0.6233	961.1	1060.8	160.7	0.6742
911.9	1036.1	184.7	0.6585	506.6	1036.4	161.5	0.6478
810.6	1030.7	185.2	0.6536	944.6	1020.3	202.6	0.6470
709.2	1024.9	185.6	0.6471	911.9	1018.4	202.7	0.6443
608.0	1018.6	185.8	0.6406	810	1012.9	202.8	0.6389
506.6	1011.9	186.0	0.6356	709.2	1007.0	203.1	0.6339
405.3	1003.9	186.4	0.6312	506.6	993.3	203.3	0.6276
608.0	1025.5	178.9	0.6477	608.0	986.7	216.6	0.6192
506.6	1019.3	179.0	0.6413	709.2	992.8	217.3	0.6243
405.3	1011.5	179.3	0.6371	911.9	1005.0	216.3	0.6362
709.2	1067.2	140.0	0.6674	810.6	999.4	216.3	0.6325
608.0	1062.1	140.1	0.6623	709.2	993.5	216.5	0.6257
506.6	1056.3	140.6	0.6574	608.0	985.7	216.8	0.6183
961.1	1060.8	160.7	0.6775	506.6	978.6	217.1	0.6129
911.9	1058.5	160.7	0.6727	911.9	979.7	239.6	0.6230
810.6	1053.9	160.8	0.6662	911.9	979.9	239.4	0.6227
709.2	1048.7	161.1	0.6602	911.9	979.9	239.4	0.6241
608.0	1042.5	161.4	0.6549	810.6	974.8	239.7	0.6162
506.6	1036.4	161.5	0.6487	709.2	967.7	239.9	0.6086
981.8	1056.9	166.0	0.6743	608.0	960.8	240.2	0.6007
911.9	1053.8	166.1	0.6712	506.6	952.3	240.1	0.5943
810.6	1048.9	166.2	0.6660	810.6	948.0	261.2	0.5966
709.2	1043.5	166.5	0.6597	810.6	948.0	261.2	0.5979
608.0	1037.2	166.8	0.6544	709.2	940.1	261.6	0.5904
506.6	1031.0	167.1	0.6486	709.2	940.1	261.6	0.5891
506.6	1043.2	154.7	0.6528	608.0	931.0	261.8	0.5812
608.0	1049.3	154.3	0.6590	608.0	931.0	261.8	0.5822
955.6	1066.9	153.3	0.6776	506.6	922.5	262.2	0.5771
911.9	1065.1	153.4	0.6761	911.9	929.9	280.8	0.5925
810.6	1060.3	153.5	0.6702	810.6	923.3	281.2	0.5839
709.2	1055.6	153.3	0.6640	810.6	923.3	281.2	0.5845
779.1	1070.8	139.8	0.6723	709.2	914.3	281.2	0.5748
786.0	1071.1	139.7	0.6723	608.0	903.3	281.2	0.5658

Table III. Thermal Conductivity Coefficients of Water (smoothed data) (10^{-5} P, N m^{-2}; T, °C; λ, W m^{-1} °C^{-1})

	T						
P	50	100	150	200	250	300	350
sat	0.640	0.670	0.677	0.659	0.613	0.549	
100	0.646	0.677	0.686	0.666	0.622	0.553	
200	0.652	0.684	0.693	0.674	0.634	0.574	0.470
300	0.657	0.691	0.700	0.682	0.646	0.592	0.506
400	0.664	0.697	0.706	0.689	0.656	0.606	0.532
500	0.669	0.703	0.714	0.696	0.665	0.618	0.551

Table IV. Thermal Conductivity Coefficients of Heavy Water (smoothed data) (10^{-5} P, N m^{-2}; T, °C; λ, W m^{-1} °C^{-1})

	T						
P	50	100	150	200	250	300	350
sat	0.620	0.633	0.622	0.587	0.540	0.484	
100	0.626	0.639	0.628	0.594	0.549	0.486	
200	0.631	0.645	0.635	0.602	0.559	0.502	0.405
300	0.637	0.651	0.642	0.610	0.568	0.515	0.436
400	0.643	0.656	0.648	0.619	0.577	0.527	0.458
500	0.648	0.661	0.654	0.626	0.585	0.538	0.477
600	0.653	0.666	0.660	0.632	0.593	0.549[a]	0.493[a]
700	0.658	0.671	0.666	0.638	0.600	0.559[a]	0.507[a]
800	0.663	0.676	0.671	0.644	0.607	0.568[a]	0.521[a]
900	0.668	0.681	0.676	0.650	0.614	0.577[a]	0.533[a]
1000	0.673	0.686	0.681	0.656	0.620	0.585[a]	0.543[a]

[a] Extrapolated values.

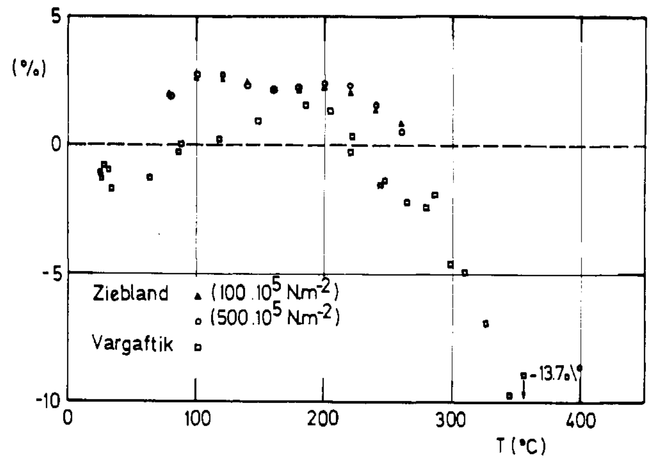

Figure 5. Percentage deviation between experimental thermal conductivity coefficients of heavy water listed in the literature and our data.

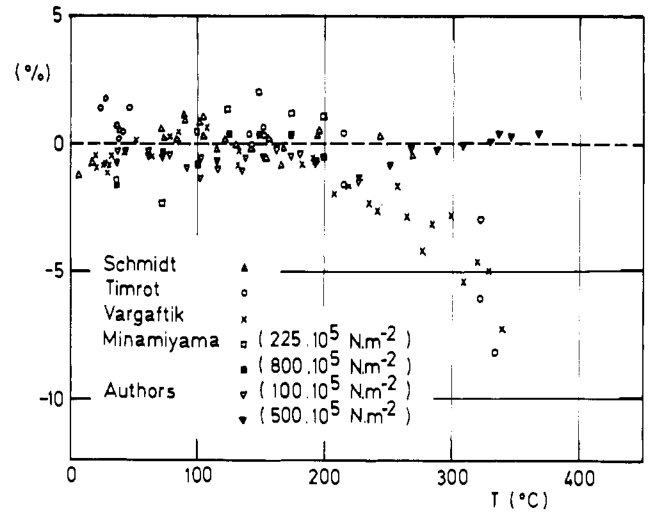

Figure 6. Percentage deviation between experimental and calculated thermal conductivity coefficients of water.

of decreasing densities show that λ/ρ increases to a maximum and then is roughly independent of the density.

The behavior of the thermal conductivity of water differs from that of other liquids only between the freezing point and the temperature corresponding to the maximum of conductivity (135 °C).

(2) Comparison of Our Results with Previous Measurements. Our results are in good agreement with literature data except in the critical region. The divergences observed with the data obtained by the hot wire method could be explained by an under estimation of the influence of the ionization in the hot wire method. Studies made with a solution of sodium chloride in water between 0 and 100 °C show that for a given concentration in NaCl the thermal conductivity coefficient decreases when the temperature increases (*14*). In the critical region our results have been discussed in a recent paper and were shown to be in good agreement with theoretical equations (*6*). On Figure 5 is shown the percentage deviation between some selected experimental thermal conductivity coefficients of heavy water listed in the literature and our data.

(3) Correlation. The general correlation for the thermal conductivity of water in the vapor phase and the critical region (*2*) was extended to the liquid phase by subtracting from the ideal conductivity

$$\lambda_{id} = \lambda(0,T) + \lambda_1 + \lambda_2\rho^2 + \lambda_3\rho^3 + \lambda_4\rho^4 \quad (8)$$

where

$$\lambda(0,T) = \sqrt{T}/(a_1 + a_2T + a_3T^2 + a_4T^4) \quad (9)$$

$\lambda_1 = 0.20165 \times 10^{-3}$ $a_1 = 1.7705414 \times 10^3$
$\lambda_2 = 1.6106 \times 10^{-6}$ $a_2 = -3.6361806$
$\lambda_3 = -1.9199 \times 10^{-9}$ $a_3 = 3.2551097 \times 10^{-3}$
$\lambda_4 = 0.9664 \times 10^{-12}$ $a_4 = -1.0598897 \times 10^{-6}$

a temperature dependent term.

$$\lambda^E = A + BT + CT_2 + DT^3 + ET^4 \quad (10)$$

where

$A = -9.8353425 \times 10^{-1}$
$B = +2.3306618 \times 10^{-3}$
$C = +3.1732809 \times 10^{-6}$
$D = -1.2203828 \times 10^{-8}$
$E = +8.3301779 \times 10^{-12}$

These last coefficients take into account the data of ref 7 and 9 up to 500 bar and the present results.

On Figure 6 is shown the percentage deviation between selected experimental data and coefficients calculated by the previous correlation.

Acknowledgment

We would like to offer our acknowledgments to Professor Johannin for his fruitful advice and stimulating discussions throughout this study.

Nomenclature

C = capacitance in pF
C_p = specific heat at constant pressure in J/(kg K)
d = gap between the cylinder in m
D = distance between the mid-points of opposite thermocouple holes in m
g = gravitational constant in m s^{-2}
G_r = Grashof number
k = thermal expansion coefficient of silver ($k = 18.9 \times 10^{-6}$ °C^{-1})
K = geometrical constant of the cell in m
P_r = Prandtl number
Q = heat flux in W
Q_{cv} = heat transfer by convection in W
Q_r = heat transfer by radiation in W
r = mean radius of the fluid layer in m
R = Rayleigh number
S = mean surface of the fluid layer in m^2
T = temperature in K

Greek Letters

α = silver emissivity coefficient
β = pressure expansion coefficient in K^{-1}
ΔT = temperature difference in K
ϵ_0 = permittivity of vacuum in F m^{-1}
ϵ_r = permittivity of air
η = viscosity in m^{-1} kg s^{-1}
λ = thermal conductivity coefficient in W m^{-1} °C^{-1}
λ_{id} = ideal thermal conductivity
λ_{measd} = measured thermal conductivity
λ_s = thermal conductivity coefficient of silver
ρ = density in kg m^{-3}
σ = Stefan–Boltzmann constant in W m^{-2} K^{-4}

Literature Cited

(1) Bridgman, P. W., *Proc. Am. Acad. Arts Sci.*, **59**, 141–169 (1923).
(2) Bury, P., Johannin, P., Le Neindre, B., Tufeu, R., Vodar, B., Proceedings

of the 8th International Conference on the Properties of Water and Steam, Editions Europeennes Thermiques et Industries, Paris, 1974, p 227.
(3) Challoner, A. R., Powell, R. W., *Proc. R. Soc. London, Part A*, **238**, 90–106 (1965).
(4) Johannin, P., Vodar, B., Wilson, H., *Prog. Int. Res. Thermodyn. Transp. Prop.*, 418 (1952).
(5) Lawson, A. W., Lowell, R., Jain, A. L., *J. Chem. Phys.*, **30**, 643–647 (1959).
(6) Le Neindre, B., Tufeu, R., Bury, P., Sengers, J. V., *Ber. Bunsenges. Phys. Chem.*, **77**, 262–275 (1973).
(7) Minamiyama, J., Yata, J., ref 2, p 243.
(8) Poltz, H., *Int. J. Heat Mass Transfer*, **8**, 515–527, 609–620 (1965).
(9) Rastorguev, I. L., Grigoryev, B. A., Ishkhanov, A. M., ref 2, p 255.
(10) Schmidt, E., Sellschopp, W., *Forsch. Ingenieurwes*, **3**, 277–286 (1932).
(11) Tarzimanov, A. A., Lozowoi, W. S., "Experimental Investigation of the Heat Conductivity of Water at High Pressures", Report C-8, 7th I.C.P.S., Tokyo, 1968.
(12) Timrot, D. L., Vargaftik, N. B., *J. Tech. Phys. (Leningrad)*, *10*, 1063 (1940).
(13) Tufeu, R., PhD Thesis, University of Paris, Paris, France, 1971.
(14) Tufeu, R., Le Neindre, B., Johannin, P., *C.R. Acad. Sci.*, **262**, 229–231 (1966).
(15) Vargaftik, N. B., Oleschuk, O. N., *Teploenergetika*, **6**, 70–74 (1959).
(16) Vargaftik, N. B., Oleschuk, O. N., Belyakova, P. E., *At. Energ.*, **7**, 465–468 (1959).
(17) Venart, J. E. S., *Adv. Thermophys. Prop. Extreme Temp. Pressures*, 3rd, 237 (1965).
(18) Ziebland, H., Burton, J. T. A., *Int. J. Heat Mass Transfer*, **1**, 242–251 (1960).

Received for review September 29, 1975. Accepted February 17, 1976.

Cohesive Energies in Polar Organic Liquids. 3. Cyclic Ketones

Edwin F. Meyer* and Carol A. Hotz
Chemistry Department, DePaul University, Chicago, Illinois 60614

Densities and vapor pressures over a range of temperatures have been measured for several cyclic alkanes and ketones. The former have been fitted to power series; the latter, to Antoine and Cox equations. Overall averages for $\Delta p/p$ are 3×10^{-4} and 2×10^{-4}, respectively, for the vapor pressure equations. Evaluation of the contributions of orientation, induction, and dispersion energies to total cohesion leads to results similar to those for the linear 2-ketones. The dipole in the cyclic ketones from C_4 through C_7 is more effective in attractive interactions than that in the 2-ketones. However, in C_8, C_{11}, and C_{12} rings, the dipole loses increasing amounts of effectiveness in attracting its neighbors, and the last one behaves as though 75% of its "polarity" has disappeared. A temperature change of 40° has very little effect on the polar interactions in the cyclic ketones.

Previous papers in this series (*11, 12*) have produced estimates of the contributions of orientation (dipole–dipole), induction (dipole-induced dipole), and dispersion (nonpolar) attractive energies to total cohesion in liquid *n*-alkyl nitriles, 2-ketones, and 1-chloroalkanes. In order to investigate the role of molecular geometry in determining these energies, we have applied our method to cyclic alkanes from C_5 to C_{12} and cyclic ketones from C_4 to C_{12}. In effect, we have repeated the work on the 2-ketones (*12*) after tying the ends of the molecules together. For an explanation of the method, the earlier papers should be consulted (*11, 12*).

Experimental Section

Vapor pressures were measured for the C_8, C_{10}, and C_{12} cyclic alkanes and the C_4, C_5, C_7, C_8, C_{11}, and C_{12} cyclic ketones with the comparative ebulliometric apparatus already described (*10*). For cycloheptane the same boiler was used, but pressures were read on a thermostated mercury manometer; for the C_{10} alkane and both of the C_{12} compounds, data were extended below the accessible range of the comparative technique using a DC 704 oil manometer (*11*).

Density and thermal expansion data were obtained for the C_7, C_8, C_{10}, and C_{12} cyclic alkanes, and for the C_4, C_7, C_8, C_{11}, and C_{12} cyclic ketones using the dilatometer already described (*19*).

The compounds were obtained from Chemical Samples Company, except for the C_{11} ketone, which was made from the C_{12} ketone following the method of Garbisch (*5*), and the C_{10} alkane, which was obtained from Pfaltz and Bauer. Compounds which were not at least 99.9% pure by gas chromatography were distilled to this minimum purity (by GLC) on a spinning band column, except the C_4 ketone, which was 99.0% pure. The single impurity had a retention time of 0.055 relative to the main peak on a DEGS column at 75 °C.

Results

The vapor pressure data were fitted to both Antoine (for convenient usage within the range of data) and Cox (for more reliable extrapolation to lower temperatures) equations (*10*). The constants with their standard deviations are presented in Tables I and II; the data upon which they are based are in Table III. The temperature of the water equilibrium (t_w) is included for those data obtained by comparative ebulliometry.

In order to increase the reliability of vaporization enthalpies calculated at temperatures below the range of the present data, the combined oil manometer and comparative ebulliometric data were fitted to the same Cox equation. Weighting of the comparative data was the same as previously described (*10*), with the standard deviation in temperature taken as 0.001 K. The manometer data were assigned equal weights, with the standard deviation in pressure taken as 0.0003 cmHg. Results of the initial data fitting showed a small systematic discrepancy between the two sets of data. Subsequent analysis of the procedure used to calibrate the oil manometer against a mercury manometer indicated that the precision of both sets of data was slightly greater than that of the calibration.

Consequently the oil manometer data were adjusted by minimizing the squares of the residuals of the combined data fit with respect to a constant factor, x, which multiplied the measured oil manometer pressures. The values of x obtained for cyclodecane, cyclododecane, and cyclododecanone were 0.9990, 0.9997, and 1.0034. The last figure is least meaningful, since the manometer thermostat was unstable during these measurements, decreasing the precision of the oil data for cyclododecanone (see Tables I and II). For another compound for which similar data were obtained, $x = 0.9996$. These results imply that our oil manometer calibrations lead to results that are